UC Davis
UC Davis Previously Published Works

Title

Laboratory performance and construction challenges for plant produced asphalt mixes containing RAP and RAS

Permalink

https://escholarship.org/uc/item/3gp9v4x1

Authors

Rahman, Mohammad
Harvey, John
Buscheck, Jeffrey
et al.

Publication Date

2023-11-01

DOI

10.1016/j.conbuildmat.2023.133082

Copyright Information

Peer reviewed
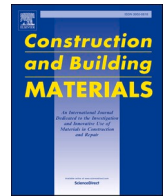
Laboratory performance and construction challenges for plant produced asphalt mixes containing RAP and RAS

Mohammad Rahman [a,*], John Harvey [a], Jeffrey Buscheck [a], Julian Brotschi [a], Angel Mateos [b], David Jones [a], Saeed Pourtahmasb [c]

[a] *University of California Pavement Research Center, Department of Civil and Environmental Engineering, University of California, Davis, One Shields Avenue, Davis, CA 95616, USA*
[b] *University of California Pavement Research Center, Institute of Transportation Studies, University of California, Berkeley, 1353 S. 46th St, Bldg. 480, Richmond, CA 94804, USA*
[c] *California Department of Transportation (Caltrans), 2389 Gateway Oaks, Suite#200, MS-91, Sacramento, CA 95833, USA*

ABSTRACT

In this study, four plant-produced asphalt mixes were considered to evaluate the performance and construction challenges of mixes containing RAP/RAS. Also, asphalt mixes were collected at two different plant-production times for each mix type to monitor the performance variability between lots. A softer base binder (PG 58–22) was used for mixes with RAS compared to the base binder (PG 64–16) used for the control mix (no RAP or RAS) and the mix with only RAP. Use of small dosages of rejuvenators and the softer binder in the RAS mixes were found to show similar performance compared to the control mix with no RAP or RAS. The results obtained from the extracted binders of these mixes indicate that mixes with RAP and RAP/RAS are expected to show higher rutting resistance and slightly lower low-temperature cracking resistance, also shown in the mix rutting and fracture cracking tests. A similar fatigue life was observed for all mixes at low strain levels in the Four-Point Beam test. However, the mix with both RAP and RAS was found to show better fatigue life at high strain levels. Similar performance test results were observed between different lots of the same mix type for most cases. Finally, there were no problems with field mixing, compaction, or finishing of the mixes containing RAP and RAP/RAS.

1. Introduction

As part of efforts toward improving environmental sustainability and reducing the life-cycle costs of asphalt pavements, various recycled materials have been used in the maintenance, rehabilitation, and construction of new pavements for more than 40 years [1,2]. Two approaches under investigation that offer the potential to advance these goals are the use of increased amounts of recycled asphalt pavement (RAP) and the use of recycled asphalt shingles (RAS) in hot mix asphalt (HMA). A survey conducted by Williams, Willis and Shacat [3] suggested that 97 million tons of RAP have been accepted by different companies in 2019. Approximately 94% of this RAP was used to construct new asphalt pavement and the remaining 6% was utilized in other civil engineering structures. In the same year, 0.92 million tons of RAS were used by the asphalt industry. The use of RAP in 2019 showed a

59.3 percent increase from the total estimated tons of RAP used in 2009. The use of these highly aged materials is helpful for asphalt mixes in terms of short-term rutting resistance and fatigue resistance in thicker asphalt layers due to an increase in stiffness [4–7]. Replacement of virgin binder in new HMA with recycled binder in RAP and RAS reduces the cost of material production because of the large differences in cost between virgin asphalt binder and RAP and RAS, which reduces life cycle costs if same or better pavement life can be achieved. Similarly, replacement of virgin aggregate and especially virgin binder can reduce mix production environmental impacts, if same or better pavement life can be achieved and if the rejuvenating agent (RA) impacts are not too high.

However, as use of RAP/RAS has increased over the years, it also has some technical concerns that can affect pavement life [1,8,9]. For example, the binder type, production location, and construction

* Corresponding author.
E-mail addresses: mohrahman@ucdavis.edu (M. Rahman), jtharvey@ucdavis.edu (J. Harvey), jcbrotschi@ucdavis.edu (J. Brotschi), angel-mateos@berkeley.edu (A. Mateos), djjones@ucdavis.edu (D. Jones), saeed.pourtahmasb@dot.ca.gov (S. Pourtahmasb).

temperature should be considered in the selection of recycling techniques [9]. A national survey conducted by Jones [10] in 2008 listed storage management, binder class, and mix properties as major issues in deciding the amount of RAP/RAS that can be safely used in new mixes. Also, an increase in RAP/RAS content was found to reduce the low-temperature cracking resistance due to addition of stiffer binders [11]. For asphalt mixes with high recycled material contents (more than 30% reclaimed binder), a suitable rejuvenator is typically used to reduce the effects of stiffer RAP/RAS binder and to increase low-temperature and block cracking resistance.

A wide variety of rejuvenators are available at this moment including engineered by-products, waste oil, aromatic extracted oil, and tall oil, as well as the use of softer virgin binder. All of these can be engineered based on their viscosity. It has been reported that better diffusivity and softening efficiency can be observed for rejuvenators with low viscosity. However, rejuvenators with high viscosity are found to show better thermal stability [12,13]. The stiffness and viscosity of old aged binder are reduced by the application of rejuvenators. However, the exact mechanism of this process is still a point of interest for researchers [14]. The effectiveness of rejuvenator also depends on the amount and type of RAP/RAS used in the asphalt mix.

The degree of blending between RAP, RAP/RAS, and virgin binders in the presence of a rejuvenator could be significant, particularly for mixes using highly aged RAP and RAS [11]. Incomplete blending could alter the properties of the mix because of less available binder and partial activation of the stiff RAP and/or RAS binder. The effects of potentially not achieving full blending need to be better understood to be effectively considered in mix design procedures and performance-related testing [11]. It is crucial that this is evaluated for real production as opposed to laboratory-produced mixes, i.e., in plant-produced mixes. These mixes subjected to silo storage undergo additional blending and aging leading to increased stiffness, improved rutting, and reduced cracking and fatigue resistance [15,16]. This outcome needs to factor into mix design procedures and specimen preparation for performance-related testing. Also, extracted binders from these mixes could be a tool to predict the performance of these hybrid mixes. However, the degree of blending between the virgin and old binder from RAP/RAS in extracted binders is 100% due to the extraction process, which may not be observed in the field. Based on that, the objectives of this study are:

- To extract and recover RAP, RAP/RAS, and RAP/RAS/virgin binder blends in assessing the effectiveness of rejuvenator.
- To characterize the extracted binder of plant-produced asphalt mixes containing RAP/RAS
- To evaluate the laboratory performance of plant-produced asphalt mixes containing RAP/RAS using performance related tests.
- To compare the performance of plant-produced asphalt mixes containing RAP/RAS from one lot to another
- To evaluate the correlation between extracted binder chemical and rheological properties, and correlation between extracted binder blend and asphalt mix laboratory performance
- To monitor the challenges in the field using asphalt mixes with RAP/RAS

2. Materials and methods

2.1. Materials

In this study, four different types of mixes with 1/2 in. nominal maximum aggregate size (NMAS) were considered to evaluate the effect of high RAP/RAS in asphalt mixes. These mixes were: (1) a control mix with no RAP or RAS (Mix A), (2) a mix with a typical amount of RAP (10%) (Mix B), (3) a mix with 3% RAS (Mix C), and (4) a mix with 10% of RAP and 3% of RAS by total weight of aggregates. A performance related non-standard special provision to the California standard

specifications was used, allowing the contractor to select the virgin base binder and type and dosage of rejuvenating agent to meet the properties of the control mix with no RAP or RAS. The mix used on the project outside of the test sections Mix B with 10% RAP. In current practice in California, no rejuvenator or change in virgin binder is required for HMA containing up to 15% RAP, and a reduction of the PG grade of the virgin binder is required for mixes with 15 to 25% RAP. RAS is not currently allowed in standard practice. A tall oil-based rejuvenator was selected by the contractor and added to Mix C and Mix D only because they contain RAS. The rejuvenator dosages for Mix C and Mix D were selected to maintain the high-performance grade (PG) of extracted binder as close to Mix A (PG 64–16) as possible. Also, an upper limit of 10% rejuvenator by the weight of total binder was maintained to ensure workability. In this study, the asphalt plant opted to choose a lower binder grade (PG 58–22) from the same binder refinery source instead of increasing the rejuvenator content and using PG 64–16 for both Mixes C and D. In the job mix formula (JMF), the rejuvenator contents found to satisfy this requirement for Mix C and D were 0.25% and 1.00% by total weight of binder. For each asphalt mix type, plant mixes were collected at two different times (lot 1 and lot 2) of mix production to evaluate the change in mix properties with the difference in plant production time. A summary of the mix composition is shown in Table 1.

2.2. Binder testing

All plant mixes were auto-extracted following ASTM D8159 in the laboratory. The extracted binder was then recovered using the rotary evaporation process following ASTM D5404. In this study, the binder was extracted from a plant-produced mix, so there were no virgin binder test results for the blend, and "plant–extracted" results are presented in place of RTFO-aged results. The chemical properties of the extracted binders were evaluated using Fourier transform infrared spectroscopy (FTIR). The spectra measured by the FTIR were recorded in a reflective mode, from 4,000 to 400 cm^{-1}, at a resolution of 4 cm^{-1}. An average value of 24 scans was recorded for each measurement. Nine replicate measurements were considered to ensure that representative measurements were collected for each binder sample. The carbonyl area (CA) index determined from FTIR was used to track chemical properties with aging. The tangential integration of the component area index was calculated between the upper and lower wavenumbers (1,671 and 1,720 cm^{-1})[17]. The aliphatic band at 2,923 cm^{-1} was used to

Table 1
A Summary of Mix Composition.

Items	Sieve size	Mix A	Mix B	Mix C	Mix D
Grading (% passing sieve)	1″	100	100	100	100
	3/4″	100	100	100	100
	1/2″	96	96	97	96
	3/8″	88	87	88	86
	#4	63	61	62	60
	#8	45	43	44	40
	#200	5.5	4.7	5.4	5.5
RAS content (% by weight of aggregate)		0	0	3	3
RAP content (% by weight of aggregate)		0	10	0	10
Base asphalt binder performance grade		64–16	64–16	58–22	58–22
Rejuvenator type		—	—	Tall Oil	Tall Oil
Rejuvenator dosage (% by weight of binder)		0	0	0.25	1.00
Binder content (% by weight of mix)		5.0	4.7	5.0	5.0
Estimated binder replacement including rejuvenator (% of total binder)		0	11.2	8.8	17.7
Number of gyrations		85	85	85	85
Air void content (%)		4.2	3.9	3.9	3.8
Voids in mineral aggregate (%)		15.7	14.8	15.5	15.7
Dust proportion		1.14	1.05	1.22	1.22

Note: RAP amount = RAP binder/ (RAP binder + virgin binder + rejuvenator). Binder replacement = (RAP and/or RAS binder + rejuvenator)/ (RAP and/or RAS binder + rejuvenator + virgin binder).

normalize the spectra and eliminate any variability introduced by the operator and any background impacts between repeat measurements. Previous literature suggested that this aliphatic band structure is not affected by aging over time [18,19]. The following equation was used to integrate the chemical component area index.

$$I_i = \int_{w_{l,i}}^{w_{u,i}} a(w)dw - \frac{a(w_{u,i}) + a(w_{l,i})}{2} \times (w_{u,i} - w_{l,i}) \tag{1}$$

where: I_i = index of area i
$w_{l,i}$ = lower wavelength integral limit of area i
$w_{u,i}$ = upper wavelength integral limit of area i
$a(w)$ = absorbance as the function of wavelength.

Rheological properties were determined with a dynamic shear rheometer (DSR). Performance grades (PG) of the extracted binders were determined following the AASHTO M320 procedure. Also, the complex shear modulus (G*) and phase angle (δ) values at four different temperatures (5, 10, 25, and 40 °C) and at 16 different testing frequencies (0.02 to 15.92 Hz) were evaluated. Using G* and δ master curves, the Glover-Rowe (GR) parameters were calculated at 15 °C temperature, and 0.005 rad/sec frequency as follows:

$$GR = \frac{G^* cos^2\delta}{sin\delta} \tag{2}$$

2.3. Mix Testing

The plant mix buckets were heated up at 135 °C for 4 h to make it workable. Then compacted specimens were prepared using a Superpave® gyratory compactor (SGC). Target air-void contents were kept at 7 ± 0.5% based on densities typically obtained in the field. The following tests were performed in the laboratory on prepared asphalt specimens:

2.4. Flexural dynamic modulus

Flexural beam frequency sweep testing was performed according to AASHTO T321 using a beam fatigue apparatus and beams prepared using a rolling wheel compactor. Specimens were tested at 10 °C, 20 °C, and 30 °C and at frequencies between 15 and 0.01 Hz. A sinewave frequency was applied to produce a tensile strain of 100 µstrain on the longitudinal surface of the beam. The measured stiffnesses and phase angles were horizontally shifted into master curves at 20 °C using Equation 3 and Equation 4.

$$log|E^*| = \delta + \frac{\alpha}{1 + e^{\beta + \gamma log\omega f_r}} \tag{3}$$

where: $|E^*|$ = magnitude of flexural dynamic modulus (MPa)
α = fitting parameter (the high asymptote of the master curve)
δ = fitting parameter (the lower asymptote of the master curve)
β, γ = fitting parameters (the slope of the transition region of the master curve)
ω = frequency (Hz)
f_r = reduced frequency, which is the shifted frequency at the reference temperature from the frequency at the test temperature (Hz)

$$logf_r = logf + log\alpha_T \tag{3}$$

where: f = frequency sweep test loading frequency (Hz)
α_T = shift factor as a function of temperature in Kelvin (°K)

The shift factor α_T was calculated by the Williams-Landel-Ferry shift function equation shown below [20].

$$log(\alpha_T) = \frac{-C_1(T - T_r)}{C_2 + (T - T_r)} \tag{5}$$

where: T = test temperature (°K)
T_r = reference temperature (°K)
C_1 and C_2 = fitting parameters

2.5. Fatigue Cracking Resistance

The AASHTO T321 was followed to evaluate the fatigue cracking resistance of plant-produced asphalt mixes. The asphalt beams were prepared using a rolling wheel compactor maintaining the air void limit of 7 ± 0.5%. Beam specimens were subjected to four-point bending by applying sinusoidal loading at three different strain levels (high, intermediate, and low) at a frequency of 10 Hz and temperature of 20 °C. The fatigue life for each strain level was selected by multiplying the maximum stiffness value for that strain level by the number of cycles at which that stiffness value occurred. In this study, the testing method currently listed in AASHTO T321 was modified to optimize the quantity and quality of the data collected. Replicate specimens were first tested at high and medium strain levels to develop an initial regression relationship between fatigue life and strain (Equation 6). Strain levels were selected, based on experience, to achieve fatigue lives between 10,000 and 100,000 load cycles at high strains and between 300,000 and 500,000 load cycles at medium strains. Additional specimens were then tested at lower strain levels selected based on the results of the initial linear regression relationship to achieve a fatigue life of about 1 million load repetitions. The final regression relationship was then refined to accommodate the measured stiffness at the lower strain level.

$$Ln(N) = A + B^*Ln(\varepsilon) \tag{6}$$

where: N = fatigue life (number of cycles)
ε = strain level (µstrain)
$A and B$ = model parameters

2.6. Rutting resistance

In this study, repeated load triaxial (RLT) tests were conducted followed by AASHTO T378 using an asphalt mixture performance tester (AMPT) to evaluate the rutting resistance of asphalt mixes. The RLT parameters assessed included flow number and the number of cycles to reach 3% and 5% permanent axial strain. To get the average value five specimens were tested from each lot of mixes. Specimens were tested with no confinement under a deviatoric stress of 483 kPa [21,22].

2.7. Indirect Tensile Cracking Resistance IDEAL-CT

In this study, IDEAL-CT testing was performed on prepared asphalt specimens followed by ASTM D8225. All specimens were conditioned at 25 °C for two hours prior to testing. Strength and CT_{index} (Equations 7 to 10) were determined as the cracking resistance parameters. It should be noted that cracking is defined here to be low-temperature and block cracking phenomena which are solely dependent on the mix properties and the environment, and not the bottom-up fatigue cracking phenomenon that depends on the interaction of traffic loading, the pavement structure, the environment, mix stiffness and fatigue cracking properties.

$$CT_{index} = \frac{t}{62} \times \frac{I_{75}}{D} \times \frac{G_f}{|m_{75}|} \times 10^6 \tag{7}$$

where: t = thickness, D = diameter, G_f = failure energy ($\frac{J}{m^2}$).

$$G_f = \frac{W_f}{D \times t} \times 10^6 \tag{8}$$

where: W_f = total area under load–displacement curve till 0.1 kN load was reached after the peak.
I_{75} = displacement at 75 %of peak load

$$|m_{75}| = \left|\frac{P_{85} - P_{65}}{I_{85} - I_{65}}\right| \tag{9}$$

where: P_{85} = of peak load

P_{65} = 65% of peak load
I_{85} = displacement at P_{85}
I_{65} = displacement at P_{65}

$$Strength, \sigma_0 = \frac{Peak\,load}{2rt} \qquad (10)$$

where: r = radius of the sample.

3. Results and discussion

3.1. Extracted binder results

It should be noted that binder extracted from mixes results in complete blending of the virgin binder, RAP binder, and rejuvenating agent and that this complete diffusion may not have occurred in the mix at the time of sampling.

3.2. Rheological properties

Fig. 1 shows the true grade temperatures for two lots of each four mixes. The true grade temperatures were consistent between the two lots for the same mix type as shown in Fig. 1. Fig. 2 shows results averaged between the lots. The results indicate that the control Mix A (0% RAP, 0% RAS) binder had the lowest average true grade high temperatures (67.9 °C), followed by Mix B (10% RAP) (72.4 °C), Mix C (3% RAS) (73.8 °C), and Mix D (10% RAP, 3% RAS) (76.2 °C). Mix C and D had a PG 58 base binder while Mix A had a PG 64 binder, but the addition of RAS (Mix C) and RAP and RAS (Mix D) resulted in Mixes C and D having high temperature true grades that were higher than those of Mix A. These results indicate that the mixes with RAP, RAS, and RAP/ RAS are expected to show better resistance to rutting than the control, Mix A, which had no RAP or RAS. The difference in high temperature grade between Mix A and Mix D is large, approximately 9 °C. Similar findings were also reported by other researchers [4,5,7,11].

For the intermediate binder true grade temperatures, Fig. 2 shows that the rank order from softest to stiffest is (1) Mix A, (2) Mix C, (3) Mix B, and (4) Mix D. The difference in intermediate temperature grade between Mix A and Mix D is approximately 4 °C. A higher intermediate binder true grade temperature indicates that the mix will be stiffer at intermediate temperatures, which for thin overlays will often produce lower fatigue and reflective cracking resistance. These results indicate that Mixes B, C, and D with RAP and RAS may have lower fatigue and reflective cracking resistance than the control Mix A in thin overlays, although Mix A has a lower high temperature true grade and poorer

rutting performance.

Fig. 2 shows that the ranking for average low temperature from lowest true grade to highest is (1) Mix A, (2) Mix C, (3) Mix B, and (4) Mix D. These results indicate that the binders with RAP and RAS were stiffer or had lower creep compliance at low temperatures than the virgin binder (Mix A). Therefore, there is a slightly higher risk of block cracking at low temperatures for Mix B and Mix D compared to Mix A. However, the difference in the low temperature true grade of Mixes B and D and that of Mix A was small, approximately 2 °C. The base binder used for Mix D was PG 58–22, whereas the base binder for Mix A was PG 68–16. Therefore, a small percentage of rejuvenator dosage (1% by weight of total binder) for Mix D showed similar low temperature PG.

The ΔTc results for 20- and 40-hour PAV-aged specimens are shown in Fig. 3 for the two lots and averaged in Fig. 4. Control Mix A had more positive ΔTc values than the mixes with RAP and RAS, and the average order from most positive to most negative is (1) Mix A, (2) Mix B, (3) Mix C, and (4) Mix D. A less negative ΔTc value (if none are positive, as is the case for these four mixes) indicates that there is less difference between the critical stiffness temperature controlling the binder true grade temperature and the critical creep compliance temperature, which indicates a better resistance to block cracking after long-term aging than does a more negative ΔTc value. In this case, the results indicate that the mixes with RAS (Mixes C and D) were more likely to have long-term block cracking than those without RAS (Mixes A and B). The difference between Mix A and Mix D for the standard 20-hour PAV aging is 2 °C, which is small, and 2.5 °C for the severe 40-hour PAV aging, which is also relatively small. In this study, the minimum specified value of −5.0 °C was considered for 20-hour PAV-aged, extracted binder in selecting the dosage of rejuvenator for mixes with RAP/RAS. As shown in Fig. 4, the average ΔTc values were greater than −5.0 °C for mixes with RAS (Mix C and Mix D). Therefore, all mixes were found to pass the ΔTc requirement after 20-hour PAV aging. Also, the variability between lots for the same mix was much higher for ΔTc values. For example, the ΔTc values observed for Mix C lot 1 and lot 2 were −2.6 °C and −4.9 °C, respectively.

Fig. 5 shows a Black Space diagram (stiffness versus phase angle) with stiffness at a reduced temperature of 15 °C and a reduced frequency of 8 (10^{-4}) Hz for three aging conditions: (1) plant extracted mix, (2) 20-hour PAV aged, and (3) 40-hour PAV aged. Imposed on the plot are the Glover–Rowe thresholds that have been identified to correlate with an increased risk of long-term aging–related block cracking [23]. Both lot samples of binder from paving are shown on the plot for the four mixes. The results show that Mix A with no RAP or RAS crosses into the transition zone only for the 40-hour PAV-aged samples. The 20-hour PAV-
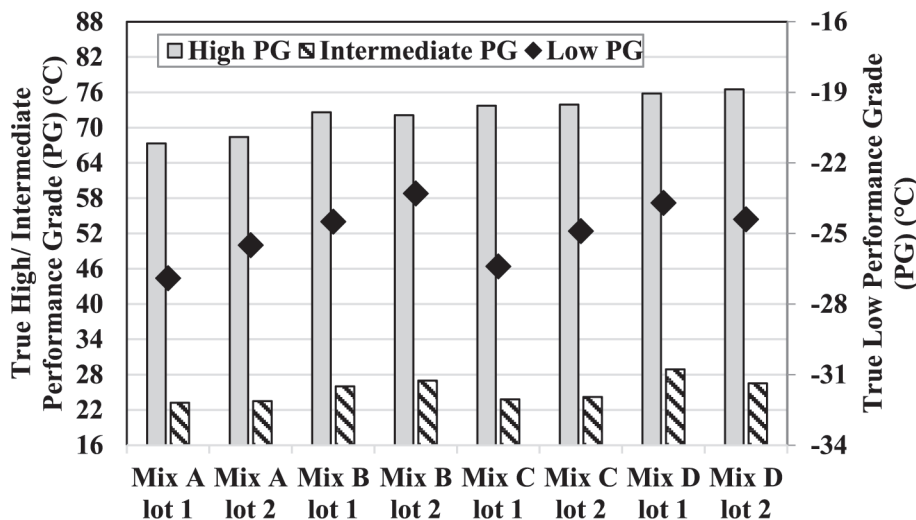

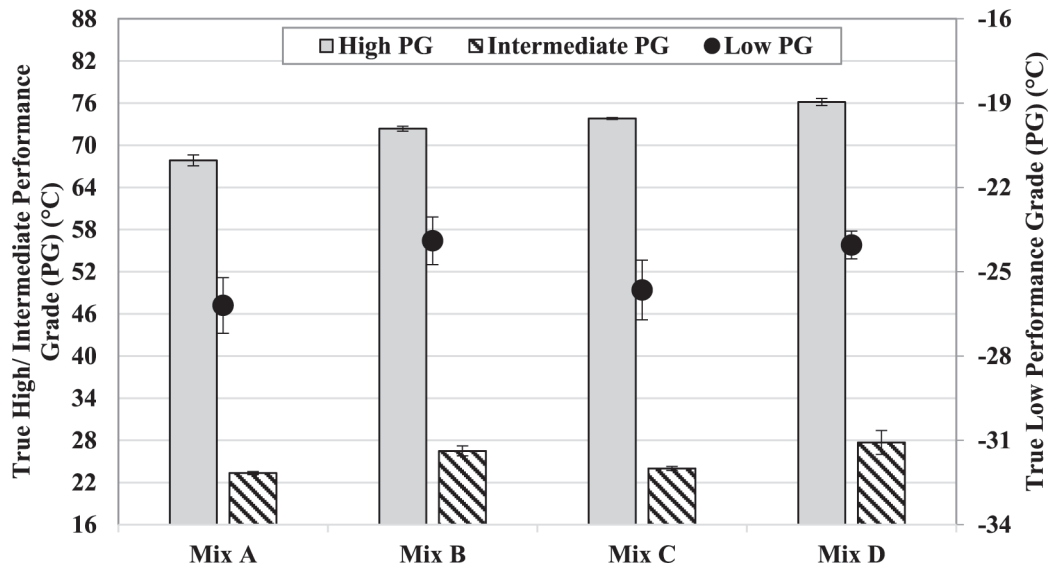**Fig. 1.** Continuous Temperature Binder Grades for All Mix Lots.

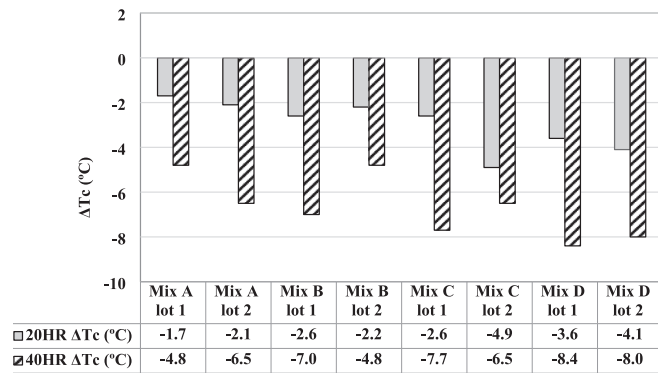**Fig. 2.** Average Continuous Temperature Binder Grades for Different Mixes.

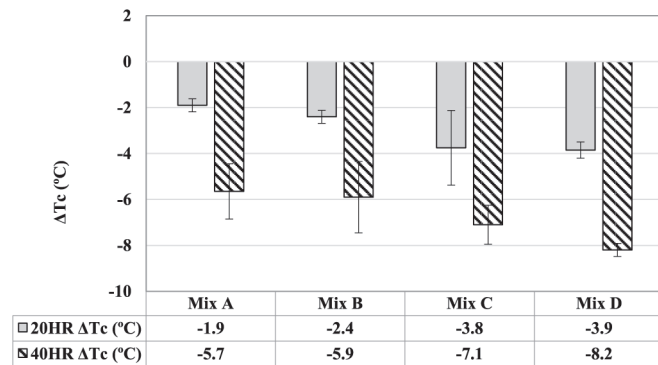**Fig. 3.** ΔTc (°C) for All Mix Lots.

Fig. 4. Average ΔTc (°C) Values for Different Mixes.

aged samples are in the transition zone for all the other three mix samples, except for one sample of Mix B. The 40-hour PAV-aged samples for Mix D show the greatest risk for block cracking with extreme aging, while the results for Mixes B and C were similar. These results indicate that Mix A has the least risk of block cracking with extreme aging, while the other three mixes, and especially Mix D, are at greater risk. Chemical properties

The extracted binders were tested with the FTIR after plant mixing and 20- and 40-hour PAV aging. Fig. 6 plots the carbonyl (CA) indices of

the binders for these three conditions for both lot samples. The results show that Mix A had the least carbonyl (aging products) after plant mixing, followed by Mix B, Mix C, and Mix D, as expected. The carbonyl contents of all four mixes increased with PAV aging, also as expected, and the results were similar between two lot samples for each mix. After PAV aging, the carbonyl indexes of Mixes B and C became more similar. Previous research shows that carbonyl content is a good indicator of the changes in binder performance indicators with different amounts of aging for rutting at high temperatures and for stiffness related to different types of cracking at lower temperatures [17,24,25]. This can be seen for the four mixes included in this project that were sampled during paving (three aging conditions each of two lots on four mixes). The results show a strong correlation between CA index and the Glover-Rowe criteria (Fig. 7 (a)), stiffness at 64 °C and 10 Hz (Fig. 7 (b)), and the crossover modulus (Fig. 7 (c)). The crossover modulus is the stiffness at which the phase angle is 45°, with decreasing crossover modulus indicating less ability to relax stresses under thermal contraction. The results show how the risk of block cracking increases with aging, the risk of rutting decreases, and the risk of low temperature cracking increases. It is interesting that the correlation remains strong despite different base binders being used in the mixes, RAP and RAS being present or not, and different dosages of the rejuvenating agent.

4. Mix Testing Results

4.1. Flexural Dynamic Modulus Frequency Sweep Results

The flexural dynamic modulus curves from the testing for Mixes A, B, C, and D with two lots are shown in Fig. 8. All the mixes have similar stiffnesses at reduced frequencies of approximately 100 Hz and faster and increasing differentiation at reduced frequencies less than 100 Hz. Below 100 Hz, Mix A is the softest, followed by Mix B in increasing stiffness, and Mixes C and D being the stiffest, although sample collected from lot 2 for Mix C is softer than Mix B lot 1 at the slowest frequencies. The relative stiffnesses are shown in Fig. 9, normalized to the lot 1 sample for Mix A, which was the softest mix at frequencies slower than 100 Hz. The results in both figures show that the results are very similar for the two lots for Mixes B, C, and D and the most variability is between the two samples for Mix A, which had no RAP or RAS.

The normalized results show that the stiffnesses of the mixes with RAS (Mixes C and D) are greater than those of the control mix with no RAS or RAP (Mix A), particularly at slow frequencies (also related to high temperatures) where rutting is an issue. These greater stiffnesses at
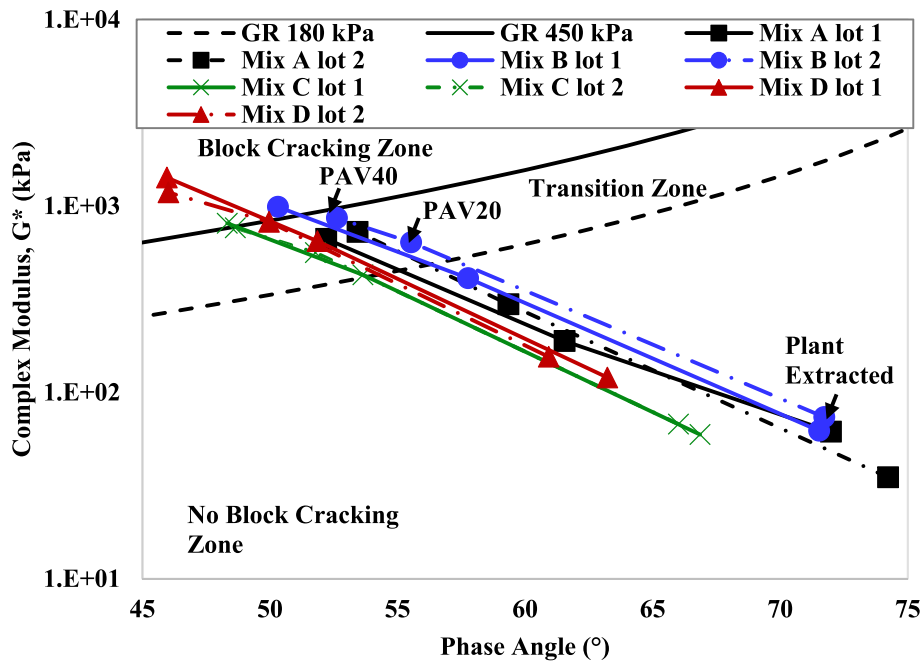
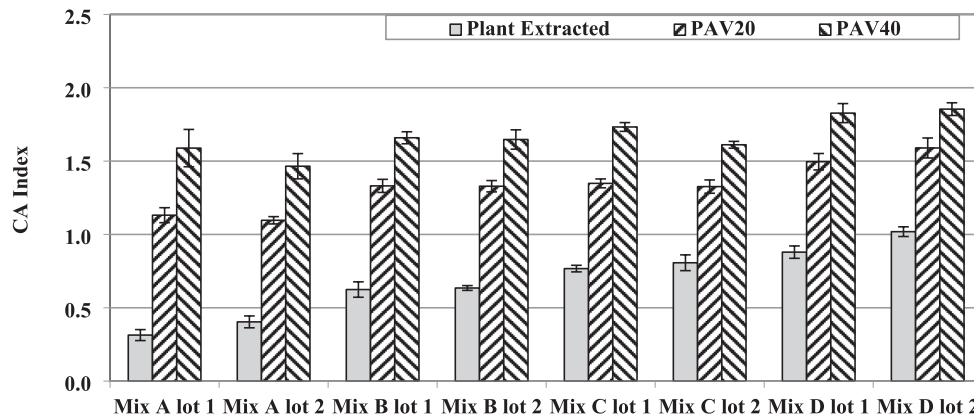**Fig. 5.** Black Space Plot for All Mixes with Glover-Rowe Criteria.

Fig. 6. Carbonyl Area (CA) Index Changes After Aging for All Mix Lots.

slow frequencies also typically result in shorter fatigue and reflective cracking lives in thin overlays and are beneficial for the same distresses in thicker overlays. The stiffness of Mix A lot 1 with no RAP/RAS is about 25% softer than the other mixes at frequencies between 1 and 100 Hz, the normal range of vehicle traffic loading times at constant speeds from boulevards to highways. These results indicate that this mix may have better fatigue and reflective cracking performance for this thin overlay project. However, Mix A lot 2 was found to show similar stiffness compared to mixes with RAP and RAP/RAS. This may be attributed due to the extended silo time in the asphalt plant causing higher stiffness for Mix A lot 2. This result indicates that differences in aging in all mixes by holding them at high temperatures in the silo prior to transporting to the laydown site, including those with or without RAP or RAS, can have an important effect on mix stiffness [15,16]. This is a common practice in many locations to improve construction logistics, and which is not addressed or is loosely addressed in most asphalt mix specifications and has not been accounted for in many research studies investigating plant-produced mix.

4.2. Rutting Resistance: Repeated Load Triaxial Test (Unconfined)

Repeated load triaxial (RLT) test results for both lots of Mixes A, B, C, and D are shown in Fig. 10; averaged across the two lots for each mix in Fig. 11. Fig. 12 shows the repetitions to 3% permanent deformation, and Fig. 13 shows the repetitions to 5% permanent deformation for the unconfined testing.

Fig. 10 and Fig. 11 show that Mix A with no RAP and no RAS has the lowest number of unconfined load repetitions to reaching a "flow" condition, indicating rapid axial permanent deformation, followed by Mixes B and D with similar results, and then Mix C, which has the best performance. The permanent axial deformation at the flow condition is similar for all four mixes as shown in Fig. 11. The unconfined RLT repetitions to 3% permanent axial strain shown in Fig. 12 indicate that rutting resistance ranked from Mix A having the worst expected performance, Mix C having the best expected performance, and Mixes B and D falling in between. These results are generally consistent with the stiffness results at slower frequencies (also related to higher temperatures). The results for unconfined RLT repetitions to 5% axial strain shown in Fig. 13 indicate the same ranking of mixes as those of the repetitions to 3% permanent axial strain.
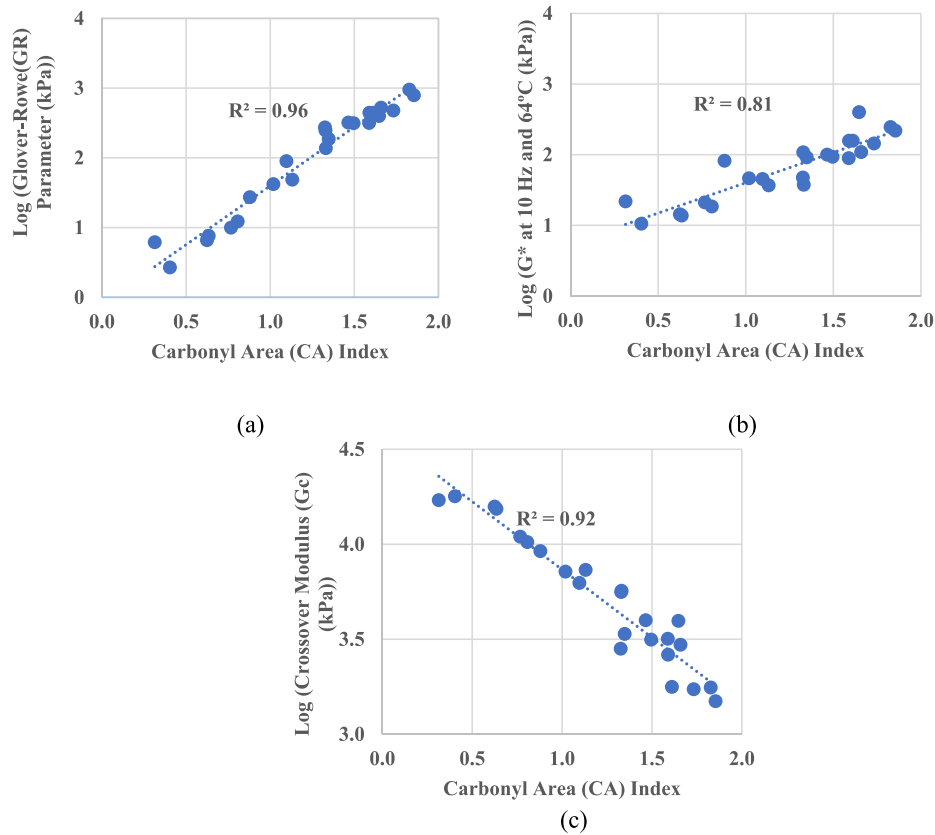
Fig. 7. Correlation Between Carbonyl Area (CA) Index and (a) Log (Glover-Rowe (GR) Parameter (kPa)) (b) Log (G* at 10 Hz and 64 °C (kPa)) (c) Log (Crossover Modulus (Gc) (kPa)).
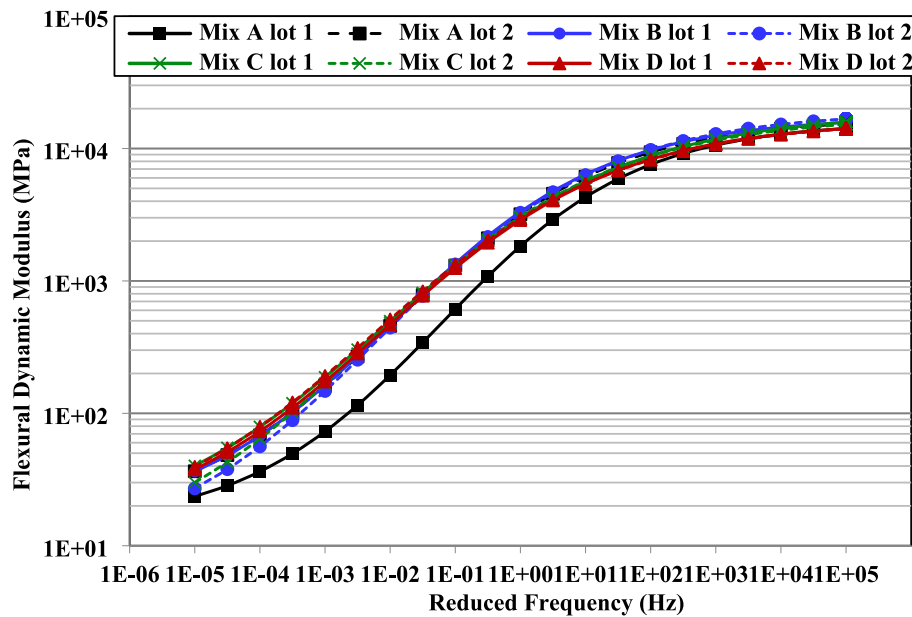

Fig. 8. Flexural Dynamic Modulus Master Curves for All Mix Lots.

4.3. Fatigue/Reflective Cracking Resistance: Four-Point Beam Test

Fig. 14 shows flexural fatigue test results for the two lot samples for each of the four mixes. Also shown on the plots are the average Wöhler curve trend lines (log of tensile strain versus log of fatigue life) for tested specimens from both lots. For the range of tensile strain levels used in testing (primarily 375 and 500 microstrain), Mix D with RAP and RAS had the best fatigue lives, followed by Mix C (RAS), Mix A (no RAP or RAS), and Mix B (RAP). These strain levels were selected to survive approximately 1 million and 250,000 cycles to failure. The ranking remained generally consistent for both lots for this tensile strain range. The higher fatigue lives for mixes with RAS might be attributed due to
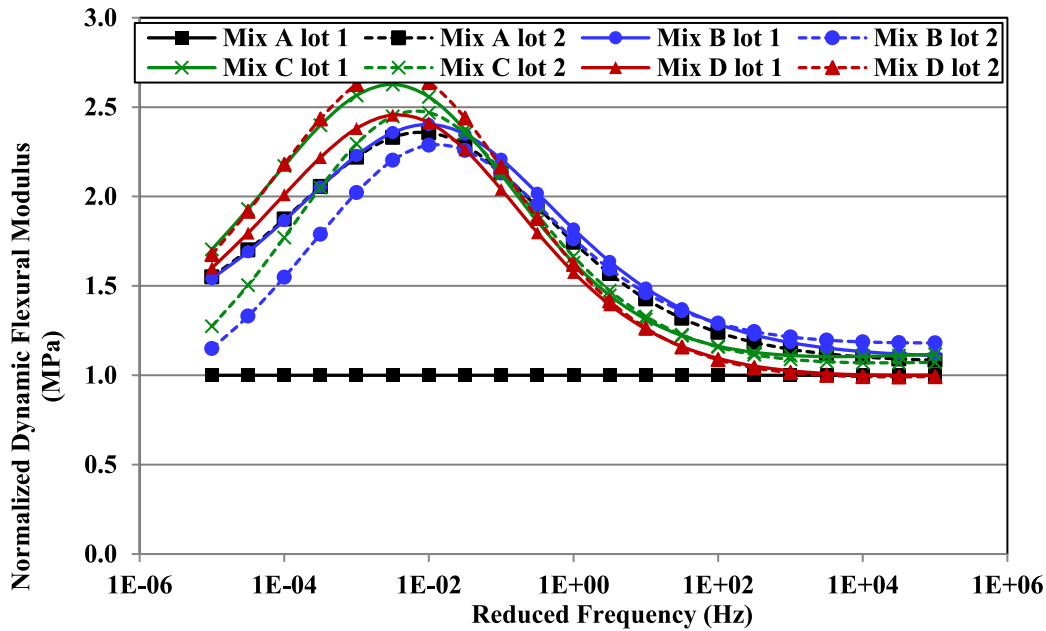
Fig. 9. Flexural Dynamic Modulus Master Curves All Mix Lots Normalized to Mix A (0% RAP, 0% RAS) First Lot.
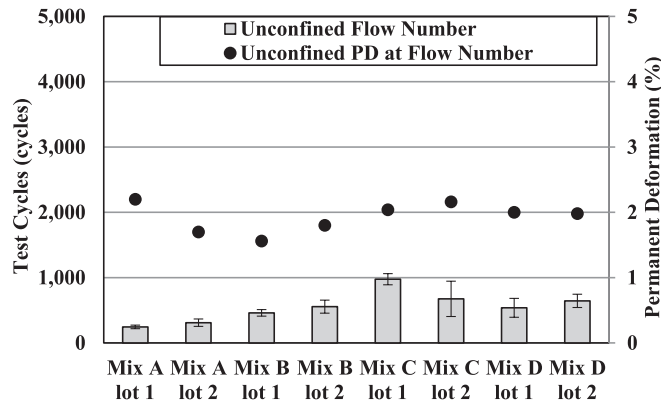

Fig. 10. Unconfined Repeated Load Triaxial Results for All Lots (Flow Number and Permanent Deformation at Flow Number).
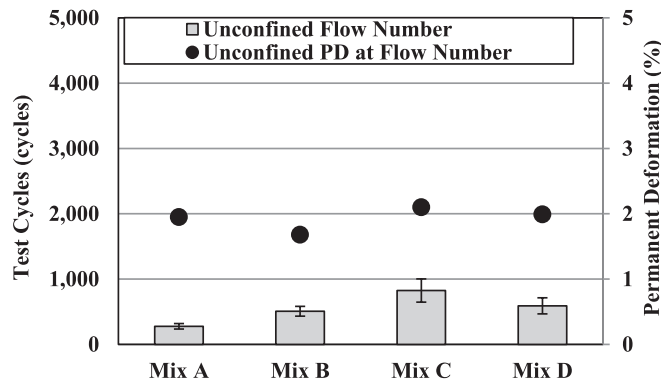

Fig. 11. Unconfined Repeated Load Triaxial Results for Different Mixes (Average Flow Number and Average Permanent Deformation at Flow Number).

the use of PG 58–22 base binder and tall-oil based rejuvenator.

The regressions from Wöhler curves have generally been found over many decades of research and practice to provide reasonable estimates when extrapolated in the approximate range of 200 to 700 microstrain,

except for polymer and rubber modified mixes that tend to have much longer fatigue lives than extrapolation would indicate at strains smaller than 200 microstrain. These results indicate that Mix A had the most sensitivity to tensile strain, with the longest fatigue life at smaller tensile strains and the shortest fatigue life at larger strains. Mix D had the flattest slope, and Mixes B and C were approximately parallel. At larger strains, typical of thin overlays on cracked pavement, Mix D has the best fatigue, followed by Mix C, and then Mixes A and B with similar fatigue performance. Tensile strains in the pavement decrease as the overlay thickness increases and mix stiffness increases in thicker overlays, and the extrapolation indicates that Mixes A and C have the best fatigue lives at small strains, followed by Mix D and then Mix B.

Fig. 15 shows flexural fatigue testing Wöhler curve results for the combined sample data sets for the four sampled mixes normalized to the results at Mix A for strain levels of 300 to 600 microstrain. The results show that at smaller strains Mixes A, C and D had similar fatigue lives, and Mix B had a lower fatigue life. The plot also shows that Mix D had a much higher fatigue life at higher tensile strain compared to other mixes.

4.4. Indirect Tensile Cracking Resistance: IDEAL-CT Test

Fig. 16 shows the IDEAL-CT results in terms of CT index and post-peak slope for the two lots of each mix, and Fig. 17 shows the same results with the results from the average of two lots. The results in Fig. 16 show large differences between the two lots for Mixes A and D and more consistent results for Mixes B and C. The variability between two lots for Mix A was also seen in the flexural stiffness results in this study, while the variability of results between samples for the IDEAL-CT test for Mix D is larger than those seen in the other tests. The average results shown in Fig. 17 indicate that Mix D has the greatest cracking tolerance, indicated by the CT index, followed by Mixes A and C with similar values, and lastly by Mix B. However, CT index values were within one standard deviation for all mixes as shown in Fig. 17. Also, the average post-peak slopes were similar for all four mixes (Fig. 17).

Fig. 18 shows the strength value (maximum stress) and fracture energy for the IDEAL-CT test for both lots for each of the four mixes. The two lots for each mix have similar fracture values, while the strength values show the greatest within-mix variability for Mixes A and C. The averaged results in Fig. 19 show similar values for strength and fracture
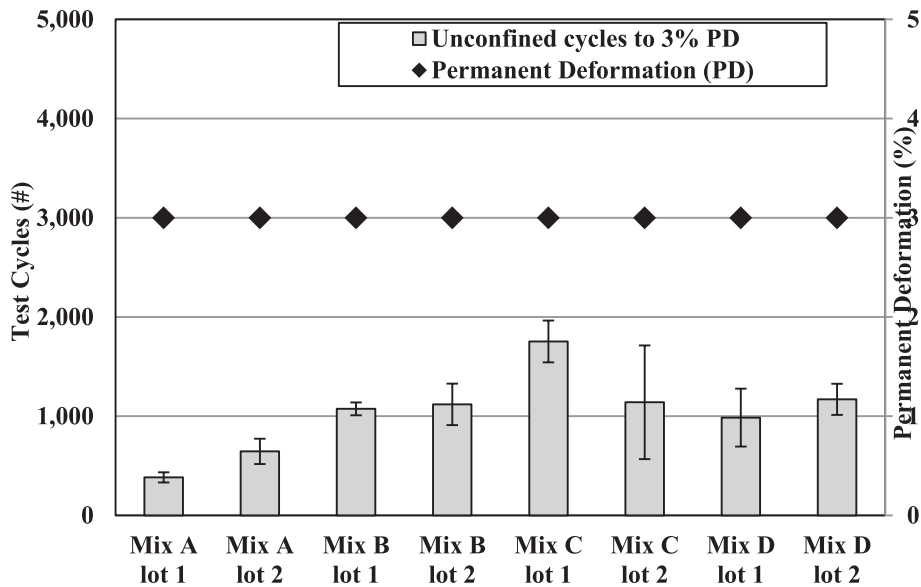
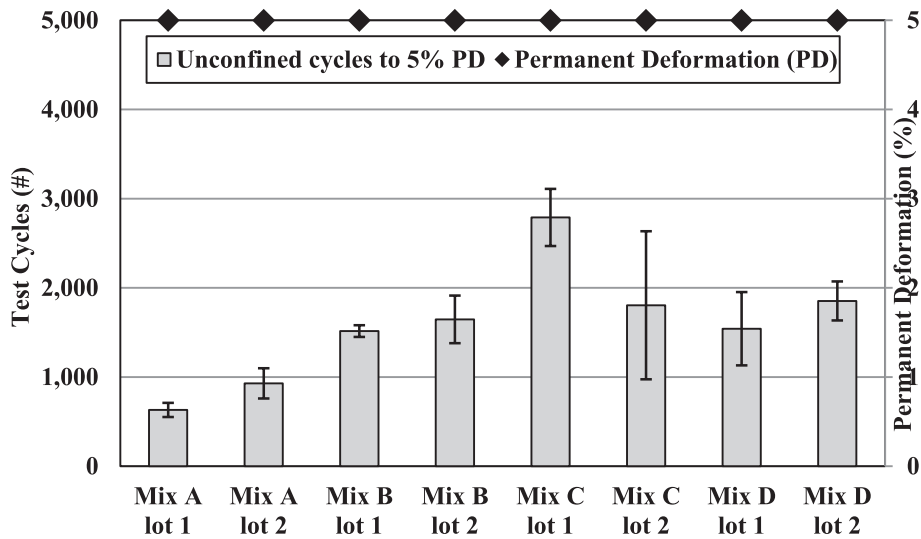**Fig. 12.** Unconfined Repeated Load Triaxial Results: Load Cycles to 3% Permanent Strain.

Fig. 13. Unconfined Repeated Load Triaxial Results: Load Cycles to 5% Permanent Strain.

energy for the four mixes, with Mix B having somewhat greater strength on average. The strength results correspond to the flexural fatigue results that showed similar stiffnesses at intermediate temperatures and intermediate loading speeds.

4.5. Extracted Binder to Mix Properties

A medium correlation (R^2 value of 0.63 to 0.65) was observed between the binder and mix parameters. The Carbonyl Area (CA) Index is expected to increase with an increase in stiffness and stiffer mixes are expected to show greater resistance to rutting. Therefore, an R^2 of 0.65 was observed between the CA index and the logarithm of flow number. An R^2 of 0.63 was observed between the CA index and the logarithm of cycles required for 5% permanent deformation (Fig. 20). However, this correlation was not very strong as shown in Fig. 20. This might be attributed to the use of different base binder (PG 58–22) for Mix C and D. Other studies suggested that the correlation between the mix and binder parameters depends on the base binder types [25]. Also, high RAP/RAS mixes without rejuvenator (stiffer mixes) were not considered in this

study. Full blending among virgin binder, aged RAP/RAS and rejuvenators is expected after forced extraction process. For plant-produced mixes, full blending may not occur during the testing. Therefore, the R^2 value was in the medium range.

4.6. Observations from the Field

There were no problems at the mixing plant that was out of the ordinary for a paving project of this type. Breakdown rolling on Mix D is shown in Fig. 21 (a). Fig. 21 (b) shows a close-up of the asphalt pavement mat after compaction for Mix D with RAP/RAS. The mat had good surface characteristics and showed no signs of segregation. The material "locked up" quickly, and paving crews indicated no problems with compaction. The temperature in the windrow was 138 °C. The lumps were soft and fell apart before going through the paver. They did not cause segregation in the mat behind the paver. The asphalt pavement constructed without RAP/RAS and with RAP/RAS will be monitored on a yearly basis to evaluate the field performance.
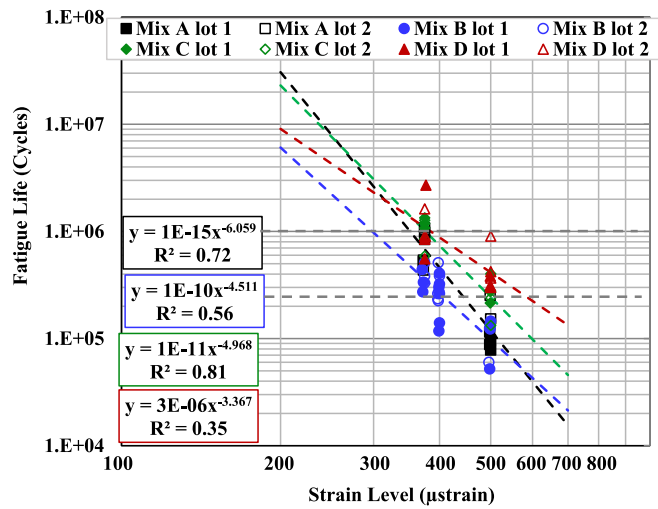
Fig. 14. Flexural Fatigue Regression Results for Different Mixes (Wohler curve).
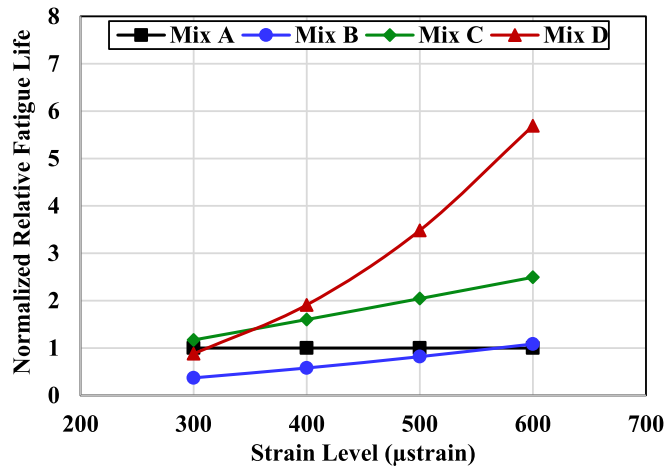

Fig. 15. Flexural Fatigue Results for Different Mixes from Wohler Curve Regression Normalized to Mix A.

5. Conclusions

In this study, four different plant produced asphalt mixes were considered to evaluate the effect of using RAP, RAP/RAS in the field. These mixes were: Mix A (control mix, without RAP/RAS), Mix B (Typical mix, 10% RAP), Mix C (3% RAS), and Mix D (10% RAP and 3% RAS). For each mix type, plant mixes were collected two different times. Based on the results, the following conclusions can be made:

• For Mixes with RAS (Mix C and Mix D) a softer base binder (PG 58–22) was considered compared to control Mix A (PG 64–16). Therefore, the amount of rejuvenator added by the total weight of binder for Mix C and Mix D were 0.25% and 1.00%, respectively. These small percentages of rejuvenators were found to show similar mix properties for Mix C and Mix D compared to control Mix A.

• The extracted binders from Mixes B, C, and D had higher high temperature true grades and somewhat higher low temperature true grades compared with the control mix. These results indicate better rutting resistance and a similar or slightly greater risk of low temperature cracking than control Mix A. Also, the ΔTc values observed for control Mix A were somewhat better than Mixes B, C, and D, indicating a somewhat lower risk of aging-induced block cracking. The control Mix A also showed lower aging indices (carbonyl area (CA) index or Glover-Rowe (GR) parameter) under extreme aging conditions, indicating better aging resistance and therefore better block-cracking resistance. However, full blending among virgin binder, aged RAP/RAS and rejuvenators is expected for Mixes B, C,
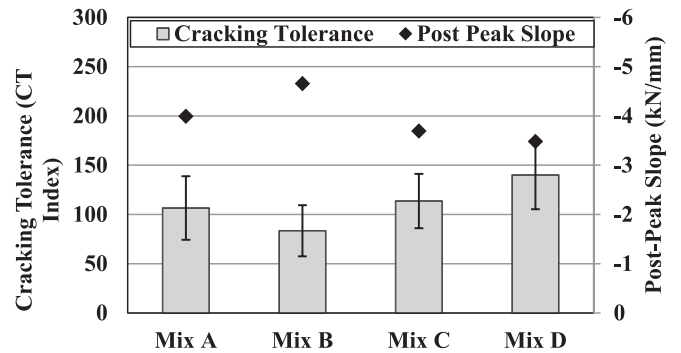

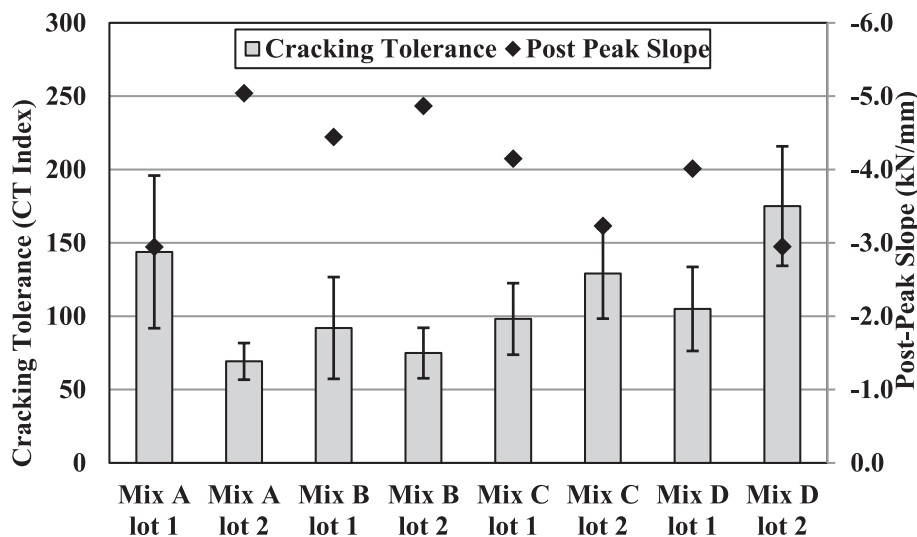**Fig. 17.** Average IDEAL-CT Test Results for All Mixes (IDEAL-CT Number and Post-Peak Slope).

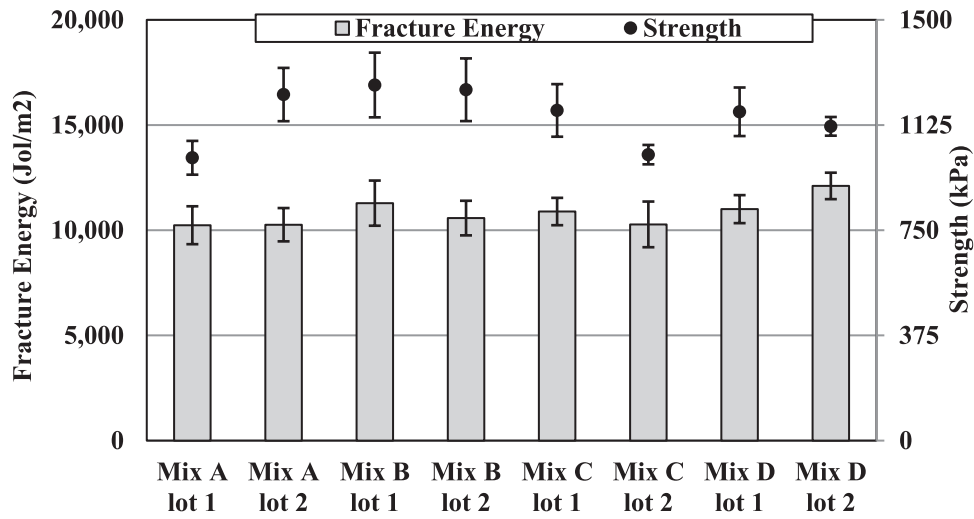**Fig. 16.** IDEAL-CT Test Results for All Mix Lots (IDEAL-CT Number and Post-Peak Slope).

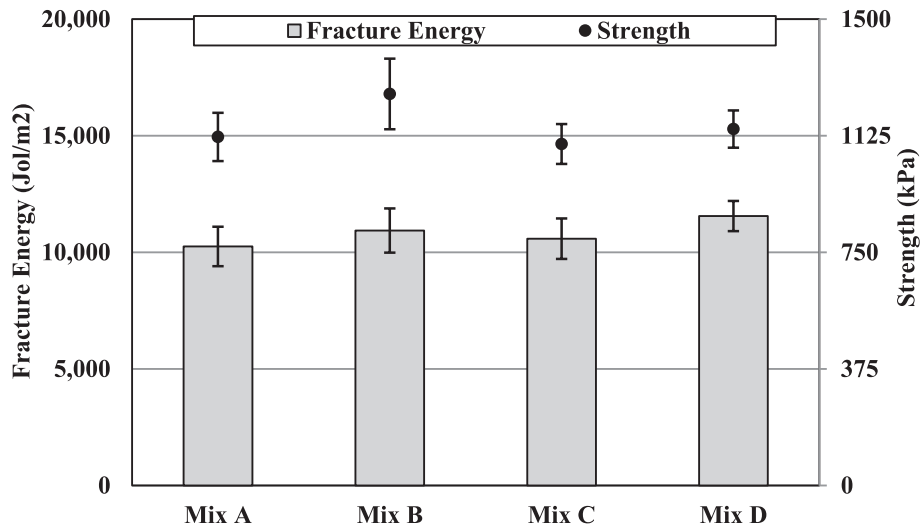**Fig. 18.** IDEAL-CT Test Results for All Mix Lots (Fracture Energy and Strength).

Fig. 19. Average IDEAL-CT Test Results for All Mixes (Fracture Energy and Strength).
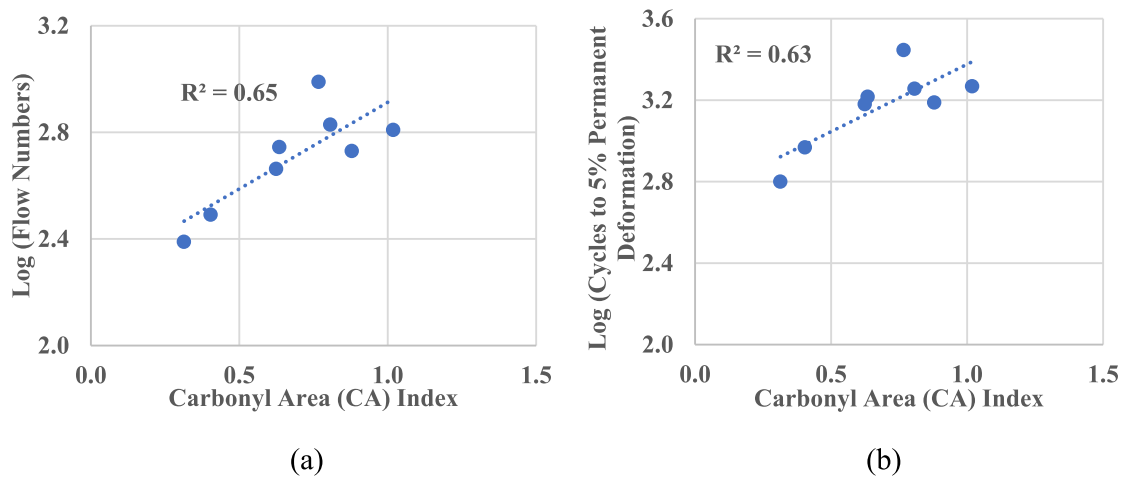

(a)

(b)

Fig. 20. Correlation Between Binder to Mix Properties ((a) Carbonyl Area (CA) Index Vs. Log (Flow Numbers) (b) Carbonyl Area (CA) Index Vs. Log (Cycles to 5% Permanent Deformation)).

Fig. 21. (a) Breakdown Rolling (b) Close-up of Compacted Surface for Asphalt Pavement with Mix D.

and D after the forced extraction process. This may be attributed to higher aging indices and a higher risk of block cracking for mixes with RAP and RAP/RAS.

- The mix results indicated that mixes with RAP and RAP/RAS showed slightly greater rutting resistance compared to control Mix A. Also, the fatigue results indicated that Mix A, C, and D were found to show similar fatigue life at a lower strain level. Therefore, mixes with and without RAP/RAS may show similar fatigue life for thick asphalt pavement. However, Mix D showed greater fatigue life at higher tensile strain. Mix B with PG 64–16 base binder and without rejuvenator was found to show lower fatigue life at both strain levels. The IDEAL-CT results indicated slightly better fracture cracking resistance for Mixes C and D compared with Mix A. Also, Mix B had the least cracking resistance among all mixes. However, the differences between the four mixes were not large. The strength values from the IDEAL-CT test showed similar values for Mixes A, C, and D, but generally showed Mix B to be somewhat stiffer.
- For the same mixes similar performance results were observed between samples collected at different plant-production times for most cases. However, slightly different performance was observed for control Mix A in flexural dynamic modulus testing and IDEAL-CT testing between two lots. Also, a slightly higher CT index was observed for Mix D lot 2 compared to lot 1. This may be attributed to the different silo times for mixes at the asphalt plant.
- The carbonyl area (CA) index was found to be a good predictor of binder stiffness, the Glover-Rowe (GR) parameter related to block cracking, and the crossover modulus related to low temperature creep with aging. However, a medium correlation was observed between the CA index and mix performance parameters. Partial blending between the virgin and aged binder from RAP/RAS might result in this medium correlation.
- There were no problems with mixing or compaction of any of the mixes. Their surfaces appeared to be similar for all mixes. The long-term field performance of these mixes will be monitored on a yearly basis.

The laboratory test results obtained in this study will be used in predicting the expected pavement life for different mixes using the mechanical-empirical design software. Then expected pavement life of mixes containing RAP and RAP/RAS will be compared with the control mix. The mixes were all tested without additional aging other than reheating for compaction of laboratory test specimens. Work is underway on a medium-term oven aging protocol to simulate differences in aging in mixes as measured using performance related tests, which is important for stiffness for consideration in structural design, fracture cracking and fatigue cracking.

CRediT authorship contribution statement

Mohammad Rahman: Conceptualization, Data curation, Formal analysis, Writing – original draft, Writing – review & editing. **John Harvey:** Conceptualization, Formal analysis, Supervision, Writing – original draft, Writing – review & editing. **Jeffrey Buscheck:** Data curation, Formal analysis, Supervision. **Julian Brotschi:** Data curation, Validation. **Angel Mateos:** Conceptualization, Supervision, Writing – original draft. **David Jones:** Conceptualization, Supervision, Writing – original draft. **Saeed Pourtahmasb:** Supervision, Writing – review & editing.

Declaration of Competing Interest

The authors declare that they have no known competing financial interests or personal relationships that could have appeared to influence the work reported in this paper.

Data availability

Data will be made available on request.

References

[1] R.S. McDaniel, R.M. Anderson, Recommended use of reclaimed asphalt pavement in the Superpave mix design method: technician's manual, National Research Council (US), Transp. Res. Board (2001).
[2] D.E. Newcomb, J.A. Epps, Asphalt Recycling Technology, Literature Review and Research Plan (1981).
[3] B.A. Williams, J.R. Willis, J. Shacat, Asphalt pavement industry survey on recycled materials and warm-mix asphalt usage: 2019, 2020.
[4] J. Harvey, C. Monismith, R. Horonjeff, M. Bejarano, B. Tsai, V. Kannekanti, Long-life AC pavements: A discussion of design and construction criteria based on California experience, International Symposium on Design and Construction of Long Lasting Asphalt Pavements, 2004, Auburn, Alabama, USA, 2004.
[5] M.A. Rahman, A. Arshadi, R. Ghabchi, S.A. Ali, M. Zaman, Evaluation of Rutting and Cracking Resistance of Foamed Warm Mix Asphalt Containing RAP, in: Civil Infrastructures Confronting Severe Weathers and Climate Changes Conference, Springer, 2018, pp. 129–138.

[6] M.A. Rahman, R. Ghabchi, M. Zaman, S.A. Ali, Rutting and moisture-induced damage potential of foamed warm mix asphalt (WMA) containing RAP, Innovative Infrastructure Solutions 6 (3) (2021) 1–11.

[7] A. Copeland, J. D'Angelo, R. Dongre, S. Belagutti, G. Sholar, Field Evaluation of high reclaimed asphalt pavement–warm-mix asphalt project in florida: case study, Transp. Res. Rec. 2179 (1) (2010) 93–101.

[8] I.L. Al-Qadi, M. Elseifi, S.H. Carpenter, Reclaimed asphalt pavement—a literature review, FHWA-ICT-07-001 (2007).

[9] M. Dinis-Almeida, J. Castro-Gomes, M. de Lurdes Antunes, Mix design considerations for warm mix recycled asphalt with bitumen emulsion, Constr. Build. Mater. 28 (1) (2012) 687–693.

[10] C. Jones, Summit on Increasing RAP Use in Pavements Sate's Perspective, North Carolina Department of Transportation, presented at Morerap conference at Auburn, AL, USA, 2008.

[11] M.A. Rahman, M. Zaman, S.A. Ali, R. Ghabchi, S. Ghos, Evaluation of mix design volumetrics and cracking potential of foamed Warm Mix Asphalt (WMA) containing Reclaimed Asphalt Pavement (RAP), Int. J. Pavement Eng. (2021) 1–13.

[12] T. Ma, X. Huang, Y. Zhao, Y. Zhang, Evaluation of the diffusion and distribution of the rejuvenator for hot asphalt recycling, Constr. Build. Mater. 98 (2015) 530–536.

[13] A. Ongel, M. Hugener, Impact of rejuvenators on aging properties of bitumen, Constr. Build. Mater. 94 (2015) 467–474.

[14] A. Behnood, Application of rejuvenators to improve the rheological and mechanical properties of asphalt binders and mixtures: a review, J. Clean. Prod. 231 (2019) 171–182.

[15] M. Elkashef, J. Harvey, D. Jones, L. Jiao, The impact of silo storage on the fatigue and cracking resistance of asphalt mixes, Constr. Build. Mater. 326 (2022), 126880.

[16] L. Jiao, M. Elkashef, J.T. Harvey, M.A. Rahman, D. Jones, Investigation of fatigue performance of asphalt mixtures and FAM mixes with high recycled asphalt material contents, Constr. Build. Mater. 314 (2022), 125607.

[17] Y. Liang, R. Wu, J.T. Harvey, D. Jones, M.Z. Alavi, Investigation into the oxidative aging of asphalt binders, Transp. Res. Rec. 2673 (6) (2019) 368–378.

[18] B. Hofko, M.Z. Alavi, H. Grothe, D. Jones, J. Harvey, Repeatability and sensitivity of FTIR ATR spectral analysis methods for bituminous binders, Mater. Struct. 50 (3) (2017) 1–15.

[19] J. Lamontagne, P. Dumas, V. Mouillet, J. Kister, Comparison by Fourier transform infrared (FTIR) spectroscopy of different ageing techniques: application to road bitumens, Fuel 80 (4) (2001) 483–488.

[20] M.L. Williams, R.F. Landel, J.D. Ferry, The temperature dependence of relaxation mechanisms in amorphous polymers and other glass-forming liquids, J. Am. Chem. Soc. 77 (14) (1955) 3701–3707.

[21] J. Harvey, A. Liu, J. Zhou, J.M. Signore, E. Coleri, Y. He, Superpave Implementation Phase II: Comparison of Performance-Related Test Results, (2014).

[22] Y. He, Interaction between New and Age-hardened binders in asphalt mixes containing high quantities of reclaimed asphalt pavement and reclaimed asphalt shingles, University of California, Davis, 2016.

[23] G. Rowe, Prepared discussion for the AAPT paper by Anderson et al.: Evaluation of the relationship between asphalt binder properties and non-load related cracking, J. Assoc. Asphalt Paving Technol. 80 (2011) 649–662.

[24] M. Liu, K. Lunsford, R. Davison, C. Glover, J. Bullin, The kinetics of carbonyl formation in asphalt, AIChE J 42 (4) (1996) 1069–1076.

[25] M.A. Rahman, J.T. Harvey, M. Elkashef, L. Jiao, D. Jones, Characterizing the aging and performance of asphalt binder blends containing recycled materials, Advances in Civil Engineering Materials 12 (1) (2023) 1–17.